Catal Lett (2008) 123:226–232
DOI 10.1007/s10562-008-9469-6

Characterization and Evaluation of Methylcyclopentane and Cyclohexane Ring Opening over Ir/ZrO_2–MoO_3 Catalysts

Zhenhui Wang · Alan E. Nelson

Received: 16 November 2007 / Accepted: 3 March 2008 / Published online: 24 April 2008

Abstract A series of Ir/ZrO_2–MoO_3 catalysts with different molybdenum concentrations and iridium loadings were synthesized and studied for ring opening of methylcyclopentane and cyclohexane to n-hexane. X-ray photoelectron spectroscopy (XPS) indicated that molybdenum and zirconium were present mainly in the form of MoO_3 and ZrO_2, respectively, and temperature programmed desorption (TPD) indicated the acidity was strongly correlated to the MoO_3 content. Iridium was incorporated by wet impregnation to a desired loading of 30 and 300 ppmw with the concentration verified by instrumental neutron activation analysis (INAA). The vapor phase conversion of methylcyclopentane and the liquid phase conversion of cyclohexane were subsequently studied to determine catalytic activity and selectivity. The Ir/ZrO_2–MoO_3 catalyst with 3.5 at.% molybdenum and 30 ppmw iridium produced an overall relatively high activity and selectivity for the conversion of cyclohexane to n-hexane.

Keywords Hydrotreating · Selective Ring Opening · Zirconium · Molybdenum · Iridium · Methylcyclopentane · Cyclohexane

1 Introduction

Hydrogenation and hydrocracking of aromatics have become proven technologies in the petroleum refining industry to address the more restrictive fuel quality standards and increased environmental legislation [1]. Diesel fuels that contain lower concentrations of aromatics have higher cetane numbers, giving shorter ignition delays, smoother engine operation, more complete combustion, and lower particulates in the exhaust gases. With the increased utilization of heavy oils and vacuum residue new catalysts are required to selectively hydrogenate the aromatics and polyaromatics of heavy oils to produce diesel fuels with lower aromatic content. The reduction of fuel aromatic content is typically accomplished using a heterogeneously catalyzed process to saturate the aromatics and subsequently cleave endocyclic C–C bonds to produce straight chain (or branched) paraffins. Although ring opening can be accomplished on either acidic or metallic catalysts, it is generally recognized that bifunctional catalysts comprised of both metallic and acidic functionality are superior to monofunctional catalysts. The acidic sites facilitate the isomerization from six-membered rings to five-membered rings, and consequently promote the ring opening on metallic sites. Solid-acid supported noble metal catalysts have been extensively studied for aromatic hydrogenation and ring opening, and several reaction mechanisms have been proposed [2–5].

Combined with a second metal oxide, zirconia (ZrO_2) has many attractive catalytic properties including a strong interaction with active phases, acidic and basic functionality, and thermal and chemical stability. Metal oxides such as MoO_3, WO_3, or CuO can be combined with ZrO_2 by wet-impregnation, sol–gel impregnation, or co-precipitation. The second metal oxide, as well as the method of preparation,

Z. Wang · A. E. Nelson
Department of Chemical and Materials Engineering,
University of Alberta, Edmonton, AB, Canada T6G 2G6

A. E. Nelson (✉)
The Dow Chemical Company, Corporate Research
and Development, Midland, MI 48674, USA
e-mail: aenelson@dow.com

can produce a zirconia-based catalyst with different chemical, physical, and catalytic properties. Previous work has shown that the incorporation of molybdenum with zirconia through co-precipitation yields mixed oxides that have a higher surface area and are more easily reduced [6–8], leading to higher catalytic activity. In addition, iridium has been shown to have high activity specifically for catalytic ring opening. McVicker et al. [2] showed that Ir/Al_2O_3 had high activity and selectivity for both cyclopentane and bicyclonaphthene ring opening, and they further noted that iridium-based catalysts are more active and selective for breaking unsubstituted C–C bonds in five-membered ring compounds compared to platinum, ruthenium, and rhodium catalysts.

In this study, a series of Ir/ZrO_2–MoO_3 catalysts were synthesized and studied for the selective ring opening of methylcyclopentane and cyclohexane to n-hexane. Catalysts were prepared and studied with molybdenum concentrations ranging from 0 to 6.7 at.% Mo and iridium loadings of 30 and 300 ppmw. The vapor phase conversion of methylcyclopentane was studied in a (proof-of-concept) pulse flow reactor, and the conversion of cyclohexane and selectivity to n-hexane was studied using a high-pressure batch reactor. The catalyst properties were correlated to activity and selectivity to understand the structure–property relationship of these catalysts

2 Experimental

2.1 Catalyst Preparation

A series of ZrO_2–MoO_3 catalysts with different molybdenum concentrations were prepared using a co-precipitation method [6]. Predetermined quantities of zirconium oxychloride ($ZrOCl_2 \cdot 8H_2O$) and ammonium heptamolybdate ($(NH_4)_6Mo_7O_{24} \cdot 4H_2O$) were dissolved in de-ionized water the resulting solution was heated and maintained at approximately 95 °C. Ammonium hydroxide (NH_4OH in H_2O) was slowly added to a final pH of 9.25 to precipitate the ZrO_2–MoO_3 metal oxide. The resulting suspension was vacuum filtered and the filter cake was washed with distilled water. The metal oxide powder was dried at 140 °C for 8 h and calcined at 500 °C for 2 h. Iridium was incorporated via wet impregnation using a standard solution of iridium (996 $\mu g\ mL^{-1}$) in 10 wt.% HCl (Sigma–Aldrich). The required amount of iridium precursor solution was determined to achieve a final iridium loading of 30 and 300 ppmw. The solution was added to the ZrO_2–MoO_3 (or γ-Al_2O_3 as a control) and the impregnated Ir/ZrO_2–MoO_3 samples were allowed to dry at ambient conditions for about 3 h, dried in an oven at 120 °C overnight, and calcined at 500 °C for 4 h.

2.2 Characterization of Ir/ZrO_2–MoO_3

X-ray photoelectron spectroscopy (XPS) was used to obtain the composition of the ZrO_2–MoO_3 support and the corresponding oxidation states of zirconium and molybdenum. XPS studies were performed using an Axis HSi 165 XPS system with a monochromatic Al Kα X-ray source (1486.6 eV). Prior to analysis approximately 50–100 mg of sample powder was evenly dispersed to form a very thin layer in a standard copper sample cup. The samples were degassed at about 5×10^{-9} Torr for about 30 min. Survey spectra were obtained from 0 eV to 1,100 eV with a pass energy of 160 eV, a dwell time of 0.1 s and a step size of 0.3 eV. For high-resolution scans, the pass energy was 20 eV, dwell time was 0.2 s, and step size was 0.1 eV. The sweep times were determined based on optimizing the signal-to-noise ratio.

Instrumental neutron activation analysis (INAA) was used to measure the iridium concentration in the catalysts due to the low iridium concentration of iridium. Analysis was performed using a SLOWPOKE II reactor (Atomic Energy of Canada Limited) at the University of Alberta. Approximately 100 mg of catalyst sample was loaded into a polyethylene sample holder, and then the sample was irradiated with the emitted delayed gamma rays detected using a hyperpure germanium (HPGe) detector. In the present study, a delayed gamma ray at 328.45 KeV of ^{194}Ir was used for analysis because of much shorter half life of ^{194}Ir (19.28 h) compared to ^{192}Ir (73.83 days). The uncertainty ($\pm 1\sigma$) for the iridium INAA measurements was 0.7–0.8 ppmw for catalysts containing 30 ppmw iridium and 5–7 ppmw for catalysts containing 300 ppmw iridium.

Ammonia temperature programmed desorption (TPD) was performed using an automated chemisorption system (AutoChem II 2920, Micromeritics). Prior to the analysis, about 150 mg of catalyst sample was degassed by flowing helium at a flowrate of 20 $mL\ min^{-1}$ while the temperature of sample was heated from r.t. to 500 °C to remove any adsorbed contaminants. The temperature was then reduced to 80 °C, and the gas was switched to 15% NH_3 in helium. NH_3 was allowed to continuously chemisorb for 30 min after which the excess ammonia was flushed out with pure helium at a flowrate of 25 $mL\ min^{-1}$. The helium flow was maintained while the temperature was increased to 500 °C and the amount of desorbing ammonia was quantified as a function of sample temperature. The procedure was repeated at different temperature ramping rates from 25 °C to 45 °C per minute to estimate the heat of ammonia desorption.

2.3 Reactivity Experiments

The chemisorption system was used as a simple pulse mode reactor to screen the relative activity of the various catalyst formulations by studying the vapor phase conversion of methylcyclopentane at 300 °C and atmospheric pressure. These studies were performed only to determine the relative activity of each catalyst composition as a function of molybdenum substitution and iridium loading for the conversion of the probe compound (methylcyclopentane), and thus, the relative product distribution and selectivities were not determined. The relative concentration of methylcyclopentane was measured with a Dycor quadropole gas analyzer, and subsequently quantified by measuring the intensity of the mass-to-charge (*m*/*z*) ratio of 41. The *m*/*z* intensities of 8 methylcyclopentane pulse injections were quantified, and methylcyclopentane conversion was calculated based on the relative intensity of the peak compared to a blank experimental run (i.e. without catalyst). The conversion is thus defined as the disappearance of methylcyclopentane.

Prior to the experiments, the catalysts were initially reduced in hydrogen using temperature-programmed reduction (TPR). For the TPR experiments, the catalyst was degassed under helium at 500 °C, cooled to 25 °C, and then heated to 500 °C at a heating rate of 10 °C min^{-1} in a in flow of 10% H_2/Ar (50 mL min^{-1}). The catalyst was cooled to 300 °C and the methylcyclopentane experiments were then performed. Liquid methylcyclopentane was vaporized at a reflux temperature of 45 °C, flask temperature of 50 °C and a loop volume of 0.13 mL, and pulse-injected at intervals of 10 min to a carrier gas of 10% H_2/Ar (10 mL min^{-1}). The conversion of methylcyclopentane was determined by performing and averaging 8 methylcyclopentane pulse injections as discussed previously.

The conversion of cyclohexane (in hexadecane) and the selectivity to n-hexane was studied in a 15 mL batch reactor. The catalysts were initially pre-reduced prior to reaction. About 120 mg of catalyst was added into a batch reactor and the reactor was pressurized with H_2 to about 700 kPa. The reactor was completely immersed in the pre-heated sand bath (500 °C) for 2 h, and then the reactor was cooled and opened in a nitrogen glove box. About 5 mL of the reactant solution (cyclohexane to hexadecane weight ratio of 1:6) was added and the reactor was then re-pressurized with H_2 to achieve a final hydrogen pressure of 7 MPa (at reaction temperature). The reactor was immersed in the sand bath at 400 °C for 8 h and after the reaction was completed the reactor was immediately quenched in water. The liquid products were collected and analyzed with a HP 5890 GC equipped with 5970 MSD and an automatic liquid sampler. The injection volume for each analysis was 1 μl with a split ratio of 50:1. The temperature of the injector and detector was maintained at 325 °C and 300 °C, respectively. Quantitative analysis of the GC spectra was facilitated by comparing the spectra of the reaction product to a series of standard GC spectra with known cyclohexane, n-hexane, and hexadecane concentrations.

3 Results and Discussion

3.1 Composition Analysis

XPS analysis was used to determine the actual molybdenum concentration and stoichiometry of the nominal ZrO_2–MoO_3 support. Binding energies for molybdenum and zirconium and the molybdenum concentration as measured by XPS for the various catalysts are summarized in Table 1. The binding energies have been corrected based on adventitious carbon assuming a C 1s binding energy of 285.0 eV. The binding energies of the Mo $3d_{5/2}$ and Zr $3d_{5/2}$ transitions were nearly constant over the compositional range investigated, and the binding energies indicate the zirconium and molybdenum are present as ZrO_2 and MoO_3. The molybdenum concentration (Table 1) is in reasonable agreement with the expected values, and the apparent discrepancy can be attributed to slight variability in sample preparation (co-precipitation).

BET surface area measurements were also performed on the Ir/ZrO_2–MoO_3 catalysts and the results are presented in Table 1. The surface area of the catalysts increased from 18.6 m^2 g^{-1} to 26.2 m^2 g^{-1} with increasing molybdenum concentration. While the overall values are lower than those reported previously for similar catalysts, the trend of increasing surface area with increasing molybdenum concentration is consistent with previous studies [9].

INAA was used to quantify the actual catalyst iridium loading, and the measured iridium concentration for each catalyst is presented in Table 2. The measured iridium concentration is in excellent agreement with the expected values (30 and 300 ppmw). Because a single batch of each catalyst composition was used throughout the entire study and the actual iridium concentration was accurately measured by INAA, the repeatability of iridium impregnation was not determined.

3.2 NH_3 TPD

Temperature programmed desorption (TPD) of ammonia was used to determine the density and strength of acidic

Table 1 XPS analysis of Ir/ZrO_2–MoO_3 catalysts and BET surface area

Theoretical Mo (at.%)	Actual Mo (at.%)	Binding energy (eV)		Surface area (m^2 g^{-1})
		Zr $3d_{5/2}$	Mo $3d_{5/2}$	
1	0.7	182.0	232.2	18.6
2	3.5	182.1	232.3	20.9
3	4.7	182.0	232.3	21.6
4	5.0	182.2	232.4	25.3
5	6.7	182.2	232.5	26.2

Table 2 Iridium concentration determined by INAA

Mo loading (at.%)	Actual Ir concentration (μg g^{-1})	
	300 ppmw level	30 ppmw level
0.0	349	32.3
0.7	247	38.2
3.5	409	34.5
4.7	340	32.7
5.0	325	31.5
6.7	336	41.8
Ir/γ-Alumina	332	37.4

sites. The ammonia TPD profiles of $Ir/ZrO_2–MoO_3$ catalysts at a desorption temperature rate of 45 °C min^{-1} are shown in Fig. 1. It can be noted that the acidic sites were mainly observed in two temperature regions. One region was very broad over a temperature range from 110 °C to 430 °C. It was assumed based on the inherent peak shape that this broad peak was the sum of (at least) two peaks with temperature maxima (T_m) at 220 °C for the weak acid sites and 370 °C for moderate acid sites. The small high temperature desorption peak corresponding to strong acid sites was at an approximate temperature of 470 °C. Kenney et al. [9] studied the acidity of $ZrO_2–MoO_3$ catalysts without iridium and reported similar TPD patterns. However, the peak temperatures were lower than those observed in this study, which may be attributed to the introduction of iridium. The presence of iridium may have altered the interaction between MoO_3 and ZrO_2 and increased the ammonia desorption temperatures.

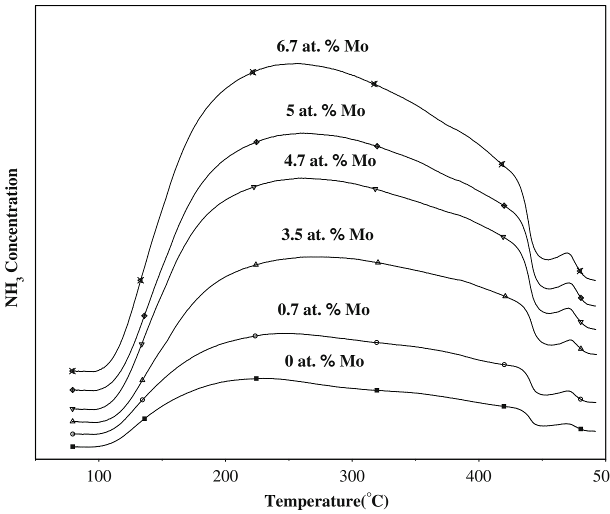

Fig. 1 NH_3 TPD profile of $Ir/ZrO_2–MoO_3$ catalysts. The TPD patterns were collected at a temperature ramp rate of 45 °C min^{-1}. Additional TPD analysis was performed using different temperature ramp rates (data not shown) to estimate the heat of ammonia desorption

The amount of ammonia desorbed corresponding to the acidic sites is given in Table 3. It was found that the total acid site density increased with molybdenum loading from 7.6 mL g_{cat}^{-1} at 0 at.% Mo to 29.4 mL g_{cat}^{-1} at 6.7 at.% Mo. Kenney et al. [9] calculated the desorbed ammonia per unit catalyst mass and unit surface area, and found that the transition from monoclinic to tetragonal structure greatly affected the acidity. The desorbed NH_3 volume decreased for monoclinic phase, and was almost constant for the tetragonal phase. The ammonia heat of desorption (ΔH_d) was calculated based on ammonia TPD data at different temperature ramp rates and is summarized in Table 4. The heat of desorption reached the maximum values of 76.3, 135.8 and 172.2 kJ mol^{-1} for weak, moderate and strong acidic sites at 3.5 at.% Mo, respectively. It should be noted that each peak identified in the study includes many acidic sites with similar but slightly different heats of desorption, which are related to the local structure of surface the acidic sites. Therefore, the calculated ammonia heats of desorption are average values for each of the supported catalysts [10].

3.3 Catalytic Reactivity

3.3.1 Methylcyclopentane Proof-of-Concept Studies

The conversion of methylcyclopentane in a pulse-flow reactor was used as an initial proof-of-concept catalyst screening test, and the measured methylcyclopentane conversions over both $ZrO_2–MoO_3$ and $Ir/ZrO_2–MoO_3$ (300 ppmw Ir) are presented in Table 5. These results clearly indicate that the introduction of iridium produced a significant increase in methylcyclopentane conversion, which can be attributed to different ring opening reaction mechanisms. For the monofunctional catalysts ($ZrO_2–MoO_3$) with acidic functionality, the reaction occurs only over acidic sites and likely follows a Haag-Dessau mechanism, as illustrated in Fig. 2. This is attributed to the absence of metallic functionality, which precludes hydrogen spillover [11] and subsequent saturation of the transitional carbenium ions. However, when iridium was incorporated ($Ir/ZrO_2–MoO_3$) it is believed that the metal function enhanced hydrogen spillover to acidic sites to form saturated products, following the classical bifunctional reaction mechanism, which further increased the conversion compared to the monofunctional catalysts.

For pure zirconia, the conversion did not increase significantly with the introduction of iridium remaining essentially zero for both ZrO_2 and Ir/ZrO_2. Thus, methylcyclopentane conversion is not only related to metallic sites but also the strength and density of acid sites. According to the present TPD results, pure zirconia possessed both the lowest number and strength of acidic sites of all catalysts studied. Methylcyclopentane conversion increased from near-zero to 75.4%

Table 3 Ammonia desorption from Ir/ZrO_2–MoO_3

Mo loading (at.%)	First T_{max} (°C)	Desorbed NH_3 (mL $gcat^{-1}$)	Second T_{max} (°C)	Desorbed NH_3 (mL $gcat^{-1}$)	Third T_{max} (°C)	Desorbed NH_3 (mL $gcat^{-1}$)
0.0	231	4.9	360	2.1	468	0.6
0.7	246	5.8	371	2.2	471	0.8
3.5	273	7.6	395	3.1	476	1.2
4.7	264	9.4	390	4.4	468	1.5
5.0	262	12.0	386	5.2	470	1.7
6.7	254	17.6	377	9.1	468	2.7

Table 4 Heat of desorption for different acid sites on Ir/ZrO_2–MoO_3 catalysts

Mo loading (at.%)	Heat of desorption (kJ mol^{-1})		
	Weak site	Moderate site	Strong site
0.0	30.8	99.2	164.4
0.7	37.0	104.2	167.1
3.5	76.3	135.8	172.2
4.7	58.3	124.3	163.3
5.0	54.1	118.6	165.6
6.7	42.9	109.2	162.1

Table 5 Methylcyclopentane conversion for Ir/ZrO_2–MoO_3 catalysts

Mo loading (at.%)	Methylcyclopentane conversion (%)		Ir concentration (ppmw)
	Without Ir	With Ir	
0.0	0.1	1.3	349
0.7	2.6	18.0	247
3.5	1.2	75.4	409
4.7	6.7	13.8	340
5.0	4.0	95.2	325
6.7	0.6	80.3	336

when the molybdenum concentration was increased from 0.0 at.% to 3.5 at.%. The increase in methylcyclopentane conversion can be attributed to the amount and strength of acidic sites as function of molybdenum loading, and specifically the heat of NH_3 desorption which experienced a mild maximum at a molybdenum concentration of 3.5 at.%. The high methylcyclopentane conversion for the catalyst containing 3.5 at.% molybdenum cannot be singly attributed to acidity, however, since the iridium loading for this catalyst was also higher (409 ppmw) than the intended iridium loading (300 ppmw) and significantly higher than the catalyst with 0.7 at.% molybdenum (247 ppmw). It should be noted that the catalyst containing 4.7 at.% molybdenum resulted in an abnormally low methylcyclopentane conversion of 13.8%. Beyond this composition the methylcyclopentane conversion increased to a maximum value of 95.2% for the catalyst containing 5.0 at.% molybdenum, and beyond this point the conversion decreased slightly to 80.3% for the catalyst containing 6.7 at.% molybdenum. As noted previously, in these initial proof-of-concept studies product selectivity was not determined.

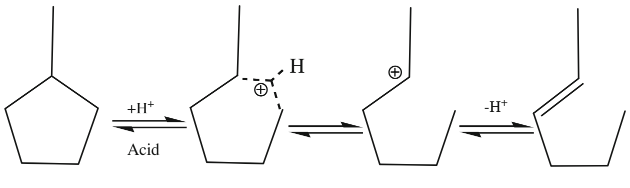

Fig. 2 Haag-Dessau ring opening reaction for methylcyclopentane over ZrO_2–MoO_3. (Adapted from Raichle et al. 2001 [12])

3.3.2 Cyclohexane Conversion and Selectivity to n-Hexane

The conversion of cyclohexane and selectivity towards n-hexane was studied using the Ir/ZrO_2–MoO_3 catalysts. An attempt was made to deconvolute the GC spectra of the product mixture to identify each product compound, but unfortunately this did not provide usable results. Thus, the selectivity in the present study is defined as the weight ratio of product n-hexane to the weight of reacted cyclohexane based on standard GC spectra with known n-hexane, cyclohexane, and hexadecane concentrations. In addition, a series of control experiments without catalyst were performed to confirm there was no reaction in the absence of the catalyst. Figures 3 and 4 summarize the relationship between cyclohexane conversion and selectivity to n-hexane for the series of catalysts, respectively.

Cyclohexane conversion (Fig. 3) slightly increased with increasing molybdenum concentration up to 5.0 at.% molybdenum. Pure zirconia produced cyclohexane conversions of 27.6% and 2.4% with 32.3 ppmw and 349 ppmw iridium, respectively, while the catalysts containing 5 at.% molybdenum produced conversions of 32.6% and 16.2% with 31.5 ppmw and 325 ppmw iridium, respectively. The catalyst containing 6.7 at.% molybdenum had slightly lower conversions of 28.7% with 41.8 ppmw iridium and 14.6% with 336 ppmw iridium. With regard to

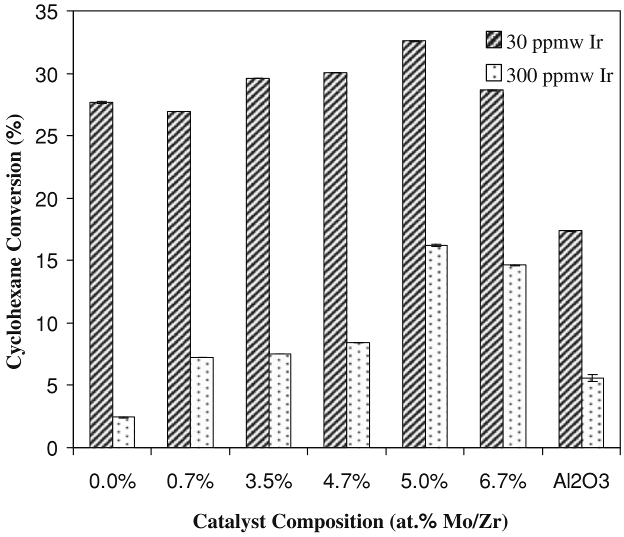

Fig. 3 Conversion of cyclohexane as function of catalyst composition (400 °C, 7 MPa H_2)

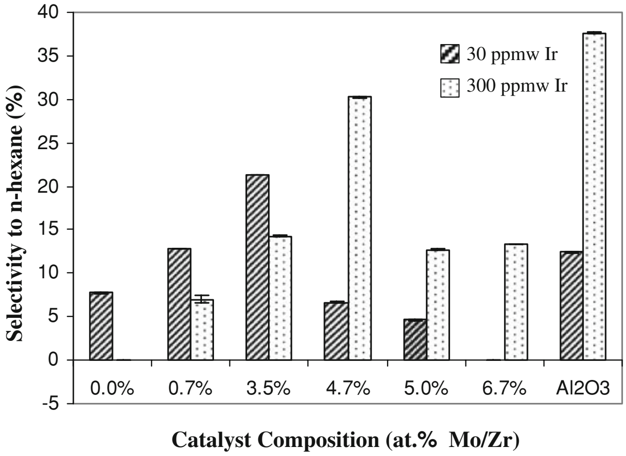

Fig. 4 Selectivity of cyclohexane to n-hexane as function of catalyst composition (400 °C, 7 MPa H_2)

iridium loading, 30 ppmw iridium catalysts produced significantly higher cyclohexane conversions than 300 ppmw iridium catalysts, suggesting that high iridium loading suppressed the activity. It should be pointed out that the total conversion includes cracking, ring opening and isomerization. Cracking almost certainly occurred under the current reaction parameters (400 °C and 8 h). In addition, high conversion tended to occur at high molybdenum concentrations (e.g. 5 at.%), where there were more acidic sites that contributed total conversion.

The selectivity for n-hexane (Fig. 4) demonstrated a similar pattern for both iridium loadings (30 and 300 ppmw) but the maximum selectivity was different for the two iridium loadings. For catalysts containing 300 ppmw iridium the selectivity reached the maximum value of 30.3% for the catalyst containing 4.7 at.% molybdenum. However, for catalysts containing 30 ppmw iridium the maximum selectivity to n-hexane was 21.3% for the catalyst containing 3.5 at.% molybdenum. The selectivity for pure zirconia was low for both iridium loadings. It is interesting to note that the selectivity to n-hexane reached the maximum value of 37.6% using the control catalyst of Ir/Al_2O_3 with 332 ppmw Ir, but the selectivity for Ir/Al_2O_3 with 37.4 ppmw iridium was considerably lower than the Ir/ZrO_2–MoO_3 catalyst at a similar iridium loading with 3.5 at.% molybdenum. This clearly illustrates the importance of balancing the metallic and acidic functionalities for maximizing activity and selectivity.

The effect of the different iridium loadings and molybdenum concentrations can be suggested from the catalyst characterization studies. According to the TPD results, the amount of acidic sites increased with increasing molybdenum loading, and the maximum heat of desorption was obtained at catalyst containing 3.5 at.% molybdenum. In the range from pure zirconia to catalysts with 4.7 at.% molybdenum, increasing acidic sites favored the selectivity to n-hexane by the presumed improvement of protonation and ring contraction steps. Beyond that point the acidic sites continued to increase, which resulted in the improvement of hydrocracking activity and lowered the yield of target products (n-hexane). According to the bifunctional mechanism, the acidic sites are not active for ring opening by themselves but greatly increase the rate of ring contraction, and metal sites also play a very important role to increase selectivity by initiating the reaction and enabling dehydrogenation/hydrogenation ability. This synergy implies higher ring opening and hydrogenation ability, which would increase the ratio of the desired product n-hexane. Additionally, it is observed (Fig. 4) that high iridium concentration does not always result in high ring opening selectivity. It can be explained that the acidic sites played a dominant role for ring opening in the compositional range in the present study.

4 Conclusions

A series of ZrO_2–MoO_3 and Ir/ZrO_2–MoO_3 catalysts with different molybdenum concentrations and iridium loadings were synthesized and characterized for the conversion of methylcyclopentane (proof-of-concept) and cyclohexane to n-hexane. The incorporation iridium significantly increased methylcyclopentane conversion to a maximum of 95.2% for a catalyst containing 5.0 at.% molybdenum and 325 ppmw iridium. The catalyst containing 4.7 at.% molybdenum and 340 ppmw iridium demonstrated the highest selectivity to n-hexane (30.3%), while the catalyst containing 3.5 at.% molybdenum demonstrated the highest selectivity to n-hexane (21.3%) for the catalysts containing

30 ppmw iridium (nominally). These catalysts compared favorably to the Ir/Al_2O_3 control catalyst, and additional studies of Ir/ZrO_2–MoO_3 catalysts to further explore the effect of molybdenum substitution and iridium loading on ring opening reactions are suggested.

Acknowledgments This work was supported by Syncrude Canada Ltd. and the Natural Sciences and Engineering Research Council (NSERC) of Canada.

References

1. Du H, Fairbridge C, Yang H, Ring Z (2005) Appl Catal A: General 294:1
2. McVicker GB, Daage M, Touvelle MS, Hudson CW, Klein DP, Baird WC, Cook BR, Chen JG, Hantzer S, Vaughan DEW, Ellis ES, Feeley OC (2002) J Catal 210:137
3. Arribas MA, Martinez A (2002) Appl Catal A: General 230:203
4. Arribas MA, Corma A, Diaz-Cabanas MJ, Martinez A (2004) Appl Catal A: General 273:277
5. Santikunaporn M, Herrera JE, Jongpatiwut S, Resasco DE, Alvarez WE, Sughrue EL (2004) J Catal 228:100
6. Calafat A, Avilan L, Aldana J (2000) Appl Catal A: General 201:215
7. Maity SK, Rana MS, Srinivas BN, Bej SK, Murali Dhar G, Prasada Rao TSR (2000) J Mol Catal A: Chemical Chemical 153:121
8. Bhaskar T, Reddy KR, Kumar CP, Murthy MRVS, Chary KVR (2001) Appl Catal A: General 211:189
9. Kenney C, Maham Y, Nelson AE (2005) Thermochimica Acta 434:55
10. Blyholder G (1964) J Phys Chem 68:2772
11. Roessner F, Roland U (1996) J Mol Catal A: Chemical 112:401
12. Raichle A, Traa Y, Fuder F, Rupp M, Weitkamp J (2001) Angew Chem Int Ed 40(7)